Molecular Biology of the Cell
Vol. 11, 1445–1455, April 2000

The Autocrine Mitogenic Loop of the Ciliate *Euplotes raikovi*: The Pheromone Membrane-bound Forms Are the Cell Binding Sites and Potential Signaling Receptors of Soluble Pheromones

Claudio Ortenzi, Claudio Alimenti, Adriana Vallesi, Barbara Di Pretoro, Antonietta La Terza, and Pierangelo Luporini*

Dipartimento di Biologia Molecolare Cellulare Animale, University of Camerino, 62032 Camerino (MC), Italy

Submitted August 30, 1999; Revised January 27, 2000; Accepted January 31, 2000
Monitoring Editor: Carl-Henrik Heldin

Homologous proteins, denoted pheromones, promote cell mitotic proliferation and mating pair formation in the ciliate *Euplotes raikovi*, according to whether they bind to cells in an autocrine- or paracrine-like manner. The primary transcripts of the genes encoding these proteins undergo alternate splicing, which generates at least two distinct mRNAs. One is specific for the soluble pheromone, the other for a pheromone isoform that remains anchored to the cell surface as a type II protein, whose extracellular C-terminal region is structurally equivalent to the secreted form. The 15-kDa membrane-bound isoform of pheromone E*r*-1, denoted E*r*-1mem and synthesized by the same *E. raikovi* cells that secrete E*r*-1, has been purified from cell membranes by affinity chromatography prepared with matrix-bound E*r*-1, and its extracellular and cytoplasmic regions have been expressed as recombinant proteins. Using the purified material and these recombinant proteins, it has been shown that E*r*-1mem has the property of binding pheromones competitively through its extracellular pheromone-like domain and associating reversibly and specifically with a guanine nucleotide-binding protein through its intracellular domain. It has been concluded that the membrane-bound pheromone isoforms of *E. raikovi* represent the cell effective pheromone binding sites and are functionally equipped for transducing the signal generated by this binding.

INTRODUCTION

Cell signaling proteins, now denoted pheromones (earlier, mating-type substances or gamones), are released by numerous species of ciliates into the extracellular environment, from where they have usually been identified and purified using bioassays based on their ability to induce a temporary shift of cells from the vegetative life to a sexual stage manifested by formation of mating pairs (for recent reviews, see Luporini *et al.*, 1995, 1996; Miyake, 1996). Consistent with this activity, it has been generally held that these proteins mediate only processes of mutual cell recognition and stimulation for mating, acting like sex factors of gametic cells (Miyake, 1981, 1996; Heckmann and Kuhlmann, 1986; Kuhlmann and Heckmann, 1989). However, experimental data derived from the study of *Euplotes raikovi*, supported by considerations on the evolution and genetics of the ciliate mating type systems, have fostered a basically different view, suggesting that ciliate pheromones primarily evolved as cell self-marker molecules (Luporini and Miceli, 1986; Luporini *et al.*, 1996; Beale, 1990). In effect, it has been shown that *E. raikovi* pheromones, in addition to inducing mating of cells via paracrine-like (or heterotypic) interactions, also bind to the same cells from which they are synthesized constitutively throughout the entire clonal life cycle (Luporini *et al.*, 1992; Vallesi *et al.*, 1995), and as a consequence of this autocrine binding they generate mitogenic signals for cell mitotic (vegetative or asexual) proliferation (Vallesi *et al.*, 1995).

This ability of *E. raikovi* pheromones to elicit varied and context-dependent cell responses is reflected in the similar three-dimensional structures of these molecules, which allow them to compete to varied extents, in vivo and in vitro, with the binding of one another (Luporini and Miceli, 1986; Ortenzi and Luporini, 1995), and of protein growth factors of animal cells such as epidermal growth factor and interleukin-2 (Ortenzi *et al.*, 1990; Vallesi *et al.*, 1998). These structures have been determined by nuclear magnetic resonance for four *E. raikovi* pheromones, E*r*-1, E*r*-2, E*r*-10, and E*r*-11 (Brown *et al.*, 1993; Luginbühl *et al.*, 1994, 1996), known to be

* Corresponding author. E-mail address: Luporini@cambio.unicam.it.

specified at a single multiallelic locus and, hence, representing homologous members of the same protein family (Raffioni *et al.*, 1992). They, in fact, all show sequences of 38–40 amino acids arranged to form a bundle of three α helices, which have an up-down-up orientation (Luginbühl *et al.*, 1994, 1996; Weiss *et al.*, 1995) and are maintained in close juxtaposition by three disulfide bonds located in conserved positions within the family (Stewart *et al.*, 1992).

However, to understand how a cell can distinguish binding of its own pheromone from binding of other pheromones and accordingly elicit one or another response, the knowledge of the structure and mechanism of action of the associated pheromone receptors is obviously a prerequisite. Studies of the structure and expression of the gene encoding pheromone E*r*-1 have strongly suggested identification of these receptors with membrane-anchored isoforms of the same diffusible pheromones (Miceli *et al.*, 1992). These isoforms are represented by type II proteins having a single transmembrane domain and their C and N termini oriented outside and inside the cell, respectively. They are generated by a mechanism of alternate splicing of the primary transcripts of the same gene that, after having been amplified to thousands of copies in the cell somatic (macro)nucleus (La Terza *et al.*, 1995), specifies the cell pheromone under a precursor form (i.e., prepro-pheromone), which is eventually processed to remove the pre and pro segments (Miceli *et al.*, 1989, 1991, 1992). Because of the genetic origin in common with the diffusible pheromone, the amino acid sequence of the membrane-bound form consists of a region that is identical to the respective prepro-pheromone sequence along with a region that is unique. The former constitutes the extracellular and transmembrane domains of the membrane-bound pheromone, the latter its cytoplasmic domain.

In this study, we have purified the protein of 130 amino acids denominated E*r*-1mem, representing the membrane-bound isoform of pheromone E*r*-1 of type I cells of *E. raikovi* (Miceli *et al.*, 1992), and expressed its extra- and intracellular domains as recombinant proteins. Using these preparations, it is shown that E*r*-1mem represents the only membrane protein of these cells that is capable of both binding competitively soluble pheromones through its extracellular domain and associating reversibly with a GTP-binding protein through the cytoplasmic one. Thus, we illustrate a case of a free-living, individual eukaryotic cell, which brings stored in a single gene the information for both of the basic molecular units of its autocrine mitogenic loop.

MATERIALS AND METHODS

Cells, Pheromones, and Chemicals

Cells used were of an offspring clone (number 39) derived from the wild-type *E. raikovi* strain number 13 (deposited at the Culture Collection for Algae and Protozoa, Ambleside, United Kingdom, under accession number 1624/18). They secrete only pheromone E*r*-1, consistent with a known homozygous combination at the genetic locus *mat* (Luporini *et al.*, 1986), and were grown on green algae *Dunaliella tertiolecta* and maintained under controlled conditions at 22–24°C. Homogeneous preparations of E*r*-1, as well as other pheromones, were obtained through standard procedures of *E. raikovi* pheromone purification (Concetti *et al.*, 1986). Routine reagents were from Sigma (St. Louis, MO), and reagents for SDS-PAGE were from Bio-Rad (Richmond, CA). Sources of other materials are specified below where appropriate.

Affinity Chromatography with Matrix-bound Er-1

The affinity matrix was prepared by linking purified preparations of E*r*-1 covalently to cyanogen bromide-activated Sepharose 4B beads (Amersham Pharmacia Biotech, Piscataway, NJ) according to the manufacturer's instructions. The final concentration of linked E*r*-1 was in the range of 1.2–1.9 mg/ml of gel slurry. The membrane preparations loaded on this affinity matrix (usually 15 mg on 1 ml of gel) were obtained using cells harvested and concentrated from cultures in an early stage of starvation, suspended with hypotonic buffer (2.5 mM Tris, pH 7.5) for 15 min in ice, and sonicated for 9 s to be lysed. Unbroken cells and nuclei were removed from lysates by centrifugation at 1000 $\times$ *g* for 1 min at 4°C. Supernatants were centrifuged at 100,000 $\times$ *g* for 30 min at 4°C, and pellets were washed twice with coupling buffer (0.1 M $NaHCO_3$, 0.4 M NaCl, pH 8.3) containing 1 mM PMSF and stored in liquid nitrogen unless immediately used. Before being used, these pellets were mixed with 1% *n*-octyl-β-D-glucopyranoside overnight at 4°C, and the mixtures were diluted with coupling buffer to 0.2% *n*-octyl-β-D-glucopyranoside, centrifuged at 100,000 $\times$ *g* for 60 min at 4°C to remove insoluble material, and incubated with E*r*-1-coupled matrix for 4 h at 4°C with gentle agitation. At the end of incubation, 0.5-ml samples of this matrix were packed in glass chromatography columns (0.5 $\times$ 10 cm), which were then washed with 20 ml of coupling buffer containing 0.2% *n*-octyl-β-D-glucopyranoside. Unless otherwise specified, elution was carried out with 1 ml of 0.1 M CH_3COONa, pH 4.0, containing 3 M NaCl, and 0.2% *n*-octyl-β-D-glucopyranoside, and the buffer of the eluted material was exchanged with Centricon-10 units (Amicon/Millipore, Bedford, MA) to 0.1 M $NaHCO_3$, pH 8.3, containing 0.2% *n*-octyl-β-D-glucopyranoside, concentrated to a final protein content of 35–55 ng/μl, and stored in liquid nitrogen before use.

Radioiodination

For E*r*-1 radioiodination, the *N*-succinimidyl 3-(4-hydroxy-5-^{125}I-iodophenyl)propionate (Bolton–Hunter reagent, 2000 Ci/mmol; Amersham, Little Chalfont, United Kingdom) was used as described earlier (Ortenzi and Luporini, 1995). The specific activity obtained for [^{125}I]E*r*-1 was in the range of 1.7–2.1 μCi/μg. For radioiodination of the affinity-purified material, Iodo-Gen reagent (Pierce, Rockford, IL) and Na[^{125}I] (100 mCi/ml, 3.7 GBq/ml; Amersham) were used as iodine sources essentially according to the manufacturer's instructions. Briefly, 20 μl of Iodo-Gen solution (0.1 mg/ml, in chloroform) were added to a 1.5-ml polypropylene tube, which was subsequently flushed with nitrogen gas until solvent was completely evaporated. The Iodo-Gen–coated tube was cooled in ice, and, in succession, 30 μl (0.5–1.0 μg) of concentrated affinity-purified material and 10 μl of Na[^{125}I] were added to it. After incubation for 30 min, this reaction mixture was transferred from the coated tube into an uncoated one containing 15 μl of 75 mM Tris and 1 M KI, pH 7.5, where it was left for 10 min at room temperature before separating the radiolabeled material from residual radioactive iodine on a Bio-Gel P-2 column (Bio-Rad) equilibrated with 75 mM Tris, pH 7.5, containing 0.2% *n*-octyl-β-D-glucopyranoside.

Binding Experiments

Samples of affinity-purified material, 100 ng in 20 μl of carbonate buffer (0.1 M $NaHCO_3$, pH 8.3) and 0.2% *n*-octyl-β-D-glucopyranoside, were applied to series of wells of a spotting manifold (Bio-Dot, Bio-Rad) assembled with a BA 85 nitrocellulose membrane (0.45-μm pore size; Schleicher & Schuell, Keene, NH), activated for 10 min in carbonate buffer, and maintained for 1 h at 4°C. After membrane saturation with 50 μl/well 5% BSA in carbonate buffer and 0.2% *n*-octyl-β-D-glucopyranoside for 1 h at 4°C, washing with 200 μl of

0.2% BSA in carbonate buffer and 0.2% *n*-octyl-β-D-glucopyranoside, and drying under vacuum, increasing amounts, in the range of 0.5–32 ng, of radioiodinated E*r*-1 were added to the duplicated samples to final volumes of 100 μl. At the end of an incubation for 1 h at 4°C, the unbound radioactivity was removed under vacuum by the addition of six volumes of carbonate buffer containing 0.2% *n*-octyl-β-D-glucopyranoside and 0.2% BSA. The membrane was then cut into small pieces, each one corresponding to one well, and the radioactivity was measured on a gamma counter (RackGamma II; LKB Instruments, Gaithersburg, MD). Nonspecific binding, defined as the radioactivity associated with the samples in the presence of a 100-fold molar excess of native E*r*-1, was subtracted from the total radioligand binding to yield specific binding.

Antibodies

Antibodies against E*r*-1 were prepared as described earlier (Miceli *et al.*, 1992), whereas antibodies against the synthetic peptide 1p25/39 (see RESULTS) were prepared by Genosys Biotechnologies (Cambridge, United Kingdom), following internal standard immunization protocols. The preparation R-3745, used in this study and denominated "anti-1p25/39," was derived from a bleeding after a total of three injections (1 mg of peptide each). Anti-GA/1 antibodies were purchased from New England Nuclear (Boston, MA), and their antigen (the synthetic peptide GA/1) was synthesized by Poiesys (Padova, Italy). Antibodies specific for conserved motifs in the C terminus of G-protein α subunits were purchased from Calbiochem-Novabiochem (San Diego, CA).

Cross-Linking and Immunoprecipitation

For chemically cross-linking [^{125}I]E*r*-1 to proteins of solubilized membrane preparations, the reagent 1-ethyl-3-(3-dimethylaminopropyl) carbodiimide hydrochloride (Pierce) was used together with the enhancer sulfo-*N*-hydroxysulfosuccinimide (final concentrations, 25 and 5 mM, respectively), and the cross-linking mixtures were gently rocked for 1 h at 4°C before being analyzed on 5–20% SDS-PAGE or exposed to immunoprecipitation with anti-1p25/39 antibodies. For immunoprecipitation, protein A-Sepharose CL-4B (Amersham Pharmacia Biotech) was prepared by swelling the lyophilized powder in 0.1 M $NaHCO_3$, pH 8.3, containing 0.2% *n*-octyl-β-D-glucopyranoside to a final concentration of 250 mg/ml, and then incubated, under gentle rocking for 2 h at 4°C, with cross-linking mixtures to which antibodies had been previously added. At the end of incubation, protein A beads were collected by centrifugation at 10,000 × *g* for 15 s at 4°C, washed sequentially three times with carbonate buffer (only initially containing 0.5 M NaCl and 0.2% *n*-octyl-β-D-glucopyranoside), suspended in SDS sample buffer containing 5% 2-mercaptoethanol, and boiled for 6 min, and the supernatants were recovered and analyzed on 5–20% SDS-PAGE.

Immunoblotting

Proteins were suspended in SDS sample buffer, in the presence of 5% 2-mercaptoethanol, boiled for 6 min, and fractionated on 5–20% SDS-PAGE. Gels were then equilibrated in 10 mM 3-(cyclohexylamino)propanesulfonic acid, 10% methanol, pH 11.0, and blotted onto polyvinylidene difluoride filters (Schleicher & Schuell) for 35 min at room temperature, under constant current of 240 mA using the same buffer. Filters were blocked with 5% BSA in 10 mM Tris, pH 7.4, 0.9% NaCl containing 0.05% Tween 20 for 4 h at room temperature and washed three times with the same buffer containing 0.1% BSA. Blocked filters were incubated with anti-E*r*-1 antibodies (working dilution, 1:2000), anti-1p25/39 antibodies (working dilution, 1:800), or anti-GA/1 antibodies (working dilution, 1:1000) in 10 mM Tris, pH 7.4, 0.9% NaCl containing 1% BSA for 12 h at 4°C. Immunocomplexes were detected by an enhanced chemoluminescence detection kit (Amersham).

Ligand Blotting

Proteins were suspended in SDS sample buffer without 2-mercaptoethanol, boiled for 6 min, and fractionated on 5–20% SDS-PAGE. Gels were then equilibrated in 25 mM Tris, pH 8.3, 192 mM glycine, 20% methanol and blotted onto BA-85 nitrocellulose filters overnight at 4°C under constant voltage of 30 V, using the same buffer. Filters were eventually blocked with 5% BSA in carbonate buffer (0.1 M $NaHCO_3$, pH 8.3), for 2 h at 4°C, washed in the same buffer containing 0.2% BSA, incubated with [^{125}I]E*r*-1 in carbonate buffer containing 1% BSA at 4°C for 12 h, washed three times with the same buffer containing 0.2% BSA, dried, and exposed to autoradiography.

ADP Ribosylation

Affinity matrix with protein linked from a membrane preparation was suspended in 20 mM Tris, pH 7.5, 100 mM NaCl, 1 mM PMSF, 2 mM $MgCl_2$, 10 mM thymidine, 1 mM ATP, and samples (500 μl each) were incubated with 10 μg of activated cholera toxin (Sigma) containing 10 μCi of [^{32}P]NAD (Amersham, 1000 Ci/mmol), for 30 min at 30°C. After addition of SDS sample buffer to arrest the reaction, samples were centrifuged, and supernatants were recovered, boiled with 5% 2-mercaptoethanol, and fractionated on 12.5% SDS-PAGE. Gels were then dried and exposed to BI imaging screens (Bio-Rad) overnight at room temperature, and the extent of [^{32}P] ADP ribosylation was quantified by a GS-250 molecular imager system (Bio-Rad).

Constructs

The plasmid p5/6, carrying the cDNA sequence of E*r*-1mem (Miceli *et al.*, 1992), was used as substrate in every PCR reaction to generate the expression vectors p143 and p3/10 containing the nucleotide sequences specific for the extra- and intracellular domains of E*r*-1mem, respectively (see Figure 1). The former sequence of 222 bp was amplified using, as forward (FW) and reverse (RV) primers, the oligos 1 M5′FW (5′-ccagtc<u>acc</u>*atg*ggatgtacatcagatctttgtc-3′) and 1 M3′RV (5′-ccagtc<u>gctcttcc</u>*gca*ggcgttggcgctgaagagtaccatagc-3′) containing introduced *Nco*I and SapI restriction sites at their respective 5′ ends (underlined letters). The latter sequence of 225 bp was amplified using the oligos 1PP5′FW (5′-ccagtc<u>cat</u>*at*gaacaaactagcaattctc-3′) and 1PP3′RV (5′-ccagtc<u>gctcttcc</u>*gca*gacataaggtgggcagttaga-3′), containing introduced *Nde*I and SapI restriction sites at their respective 5′ ends (underlined letters). An atg start codon (italicized) was included into the *Nco*I and *Nde*I sites, and the nucleotides gca (italicized) were included, as anticodons for Cys (the first amino acid residue of the intein sequence), into the 5′ end of RV primers. A tail of six extra nucleotides (ccagtc) was added to the 5′ end of each oligo to improve the efficiency of the enzymatic digestion at the restriction sites. After digestion, both the 222 and the 225 bp PCR products were ligated into the vectors pCYB3 and pCYB1 (IMPACT I kit; New England Biolabs, Beverly, MA), respectively. The constructions were checked for correct in-frame insertion with the gene encoding the intein-chitin binding domain (intein-CBD) by DNA sequencing according to standard procedures.

Bacterial Protein Expression

Transformed *Escherichia coli* cells (strain ER 2267, New England Biolabs) were grown at 37°C in Luria–Bertani broth medium containing 100 μg/ml ampicillin (Boheringer Mannheim, Indianapolis, IN), to 0.6 OD_{600}, where they were induced with 1 mM isopropyl-β-D-thiogalactopyranoside (Calbiochem-Novabiochem), for 15 h at 15°C before being harvested and stored at −20°C. Frozen cells were thawed, suspended in lysis buffer (20 mM Tris, pH 8.0, 0.9 M NaCl, 0.1 mM EDTA, 1 mM PMSF, 0.25% Triton X-100), and lysed by sonication. After incubation for 20 min, cell lysates were cleared by centrifugation at 15,000 × *g* for 30 min at 4°C, and supernatants were loaded on chitin columns (New England, Biolabs) equilibrated

with lysis buffer. Columns were washed extensively with lysis buffer, equilibrated with cleavage buffer (20 mM Tris, pH 8.0, 0.1 mM EDTA, 50 mM DTT), and incubated for 12 h at 4°C, before being eluted with cleavage buffer containing 6 M guanidine hydrochloride. Eluted material was then dialyzed and purified by reversed phase chromatography on a C_4 column (Supelcosil LC-304, 4.6 × 250 mm; Supelco, Bellefonte, PA) with a 2-propanol linear gradient (0–60% in 60 min), at a constant flow of 0.2 ml/min.

Affinity Chromatography with Chitin-bound Recombinant p3/10

Chitin columns containing p3/10 linked to intein-CBD molecules were equilibrated with washing buffer (20 mM Tris, pH 7.5, 0.1 M NaCl, 0.1 mM EDTA, 1 mM PMSF) containing 0.1% Triton X-100 immediately before being loaded with membrane preparations previously solubilized, for 3 h at 4°C, in 20 mM Tris, pH 7.5, 0.4 M NaCl, 1 mM DDT, 1 mM PMSF, 2.5% Triton X-100, diluted to 0.1% Triton X-100 with washing buffer, and centrifuged at 100,000 × *g* for 60 min at 4°C. Columns were then washed with washing buffer containing 0.1% Triton X-100, and eluted with 0.1 mM GTP, 0.5 mM $MgCl_2$, 0.1% *n*-octyl-β-D-glucopyranoside. Eluted material was concentrated with Centricon-10 units and suspended in SDS sample buffer until used.

Pheromone Coordinates

The atomic coordinates of *E. raikovi* pheromones were from the Research Collaboratory for Structural Bioinformatics (Rutgers State University, Piscataway, NJ; http://www.rcsb.org/pdb/). The identification codes for E*r*-1, E*r*-2, E*r*-10, and E*r*-11 are 1ERC, 1ERD, 1ERP, and 1ERY, respectively.

RESULTS

Primary Structure of Er-1mem

The amino acid sequence of E*r*-1mem of 14,445 Da, as deduced from its encoding nucleotide sequence (Miceli *et al.*, 1992) (GenBank–European Molecular Biology Laboratory database, accession number M86864), is shown in Figure 1, together with indications of traits of its structure that are relevant in the context of this work.

Identification of a 15-kDa Membrane Protein as Er-1mem

Studies of pheromone binding kinetics had previously shown that the highest concentrations of pheromone binding sites (i.e., 3–5 × 10^7 per cell, equivalent to 1100–1700/μm^2 of cellular surface) are expressed by type I cell cultures that, after several days of proliferation in the presence of food, are left to enter a stationary phase of growth and arrest their cycle in G_1–G_0 stage (Ortenzi *et al.*, 1990; Ortenzi and Luporini, 1995). Thus, E*r*-1mem purification was undertaken from such cell cultures, initially through two procedures. One was based on a sequence of gel filtration and ion exchange chromatography, the other on affinity chromatography with matrix-bound E*r*-1. In neither case, however, did final preparations appear homogeneous for a single protein species. Any attempt to separate the components of these preparations and carry out their direct chemical analysis systematically failed, essentially because of formation of insoluble precipitates upon concentration and detergent removal. Here we describe only results obtained from affinity chromatography, because they were more reproducible with regard both to pheromone binding activity and number of components, usually represented by 1–2 μg of protein purified 1000- to 1100-fold from starting membrane preparations of ~70 mg obtained from 50–60 × 10^6 cells.

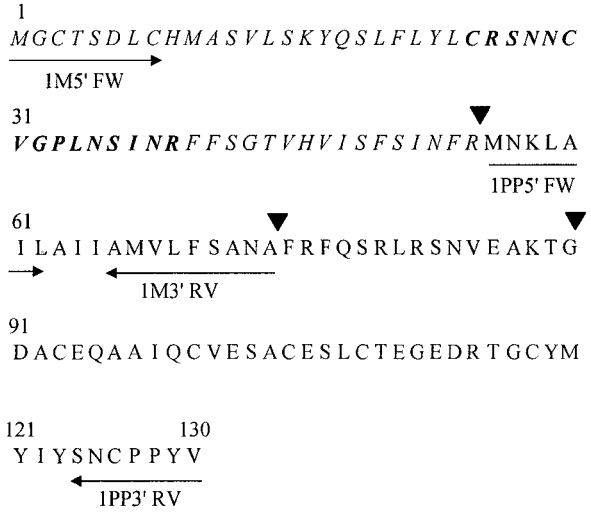

Figure 1. Sequence analysis of E*r*-1mem. The sequence of E*r*-1mem that is unique and forms its intracellular domain is printed in italics to distinguish this region from the other region, which is equivalent to E*r*-1 precursor (i.e., prepro-E*r*-1) and forms the transmembrane and extracellular domains of E*r*-1mem. Within prepro-E*r*-1, arrowheads delimit pre-, pro-, and E*r*-1. Arrows and relative denominations localize segments identified for synthesizing oligonucleotides used, as forward and reverse PCR primers (right and left orientation, respectively), for producing recombinant proteins p3/10 and p143 of E*r*-1mem. Residues in bold identify the potentially immunogenic segment, as revealed by the program PROTEAN (DNASTAR, Madison, WI), taken as reference to generate anti-1p25/39 antibodies.

In Figure 2 are reported data from binding assays of [^{125}I]E*r*-1 (prepared with the Bolton–Hunter reagent, which does not alter the pheromone bioactivity) to this affinity-purified material as a function of the ligand concentrations. They show that saturation is reached with pheromone concentrations of >68 nM, and Scatchard analysis indicates that the affinity material has a binding capacity of 1.88 × 10^3 fmol of [^{125}I]E*r*-1/μg, with a fraction of nearly 3% (calculated from a E*r*-1mem mass of 14,445 Da), able to bind the ligand with an apparent K_d of 5.3 ± 0.3 × 10^{-9} M. This is a value of the same order as that previously calculated for [^{125}I]E*r*-1 binding to intact cells (Ortenzi *et al.*, 1990; Ortenzi and Luporini, 1995).

The protein components of this material were determined after radioiodination with a tyrosine-directed method and analysis by SDS-PAGE and autoradiography. As shown in Figure 3A, these components appear as two prominent species of 55 and 15 kDa, usually accompanied by two other minor and more occasional bands of 40 and 12 kDa.

The identification of which of these proteins represented E*r*-1mem in the affinity material was based on the use of two different antibodies, both capable of recognizing specifically a unique component of ~15 kDa in immunoblot analysis of membrane preparations (our unpublished results). One, raised against E*r*-1 (Miceli *et al.*, 1992), was specific for the

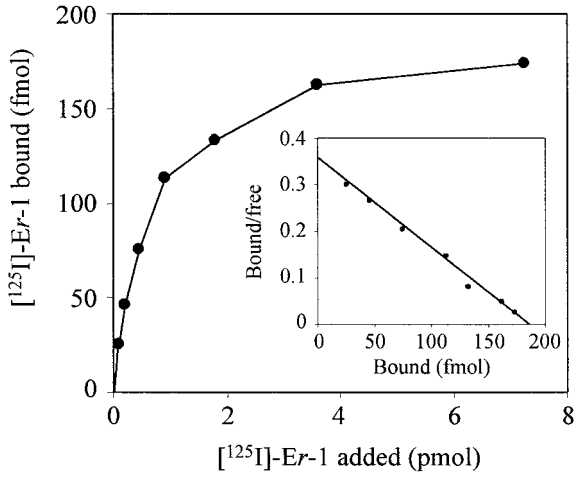

Figure 2. Concentration dependence binding of [^{125}I]E*r*-1 to affinity-purified material and plot of the binding data according to Scatchard. Each value is the mean of duplicate determinations from one experiment taken as representative and represents specific binding. Nonspecific binding was in the range of 28–48% of total binding.

E*r*-1-like extracellular domain of E*r*-1mem. The other was directed to the cytoplasmic domain of E*r*-1mem, because it was raised against a synthetic peptide, denoted 1p25/39, constructed with a sequence identical to that of a 15-amino-acid segment (Cys^{25}-Arg-Ser-Asn-Asn-Cys-Val-Gly-Pro-Leu-Asn-Ser-Ile-Asn-Arg^{39}) identified as potentially immunogenic in the N-terminal region of E*r*-1mem (see Figure 1).

In Figure 3B, the results from immunoblot analysis of affinity material show that both antibodies recognize the protein responsible for the 15-kDa band, which in effect is the unique and best candidate to represent E*r*-1mem because of the close match of its apparent molecular mass with that of 14,445 Da of E*r*-1mem (Miceli *et al.*, 1992). The specificity of this double immunorecognition was proven by the fact that this protein, hereafter denoted p15, did not bind anti-E*r*-1 antibodies in the presence of E*r*-1 or anti-1p25/39 antibodies in the presence of the peptide 1p25/39.

Pheromone Binding to p15

To assess the pheromone binding capacity of p15, samples of affinity-purified material were directly probed with [^{125}I]E*r*-1 in ligand blotting. As shown in Figure 4A, one prominent band was constantly revealed by autoradiography of the blotted filters. However, it was occasionally accompanied by a second much less intense band lying closer to the dye front. Neither band was visualized by autoradiography of filters probed with [^{125}I]E*r*-1 together with an excess of E*r*-1, or other pheromones such as E*r*-2 known to be effective as competitors of E*r*-1 binding, or incubated with anti-E*r*-1 antibodies. Thus, it was deduced that they are both specific, one being generated by [^{125}I]E*r*-1 binding to p15 and the other by [^{125}I]E*r*-1 binding to a second minor species of p15, of which we now know the existence from other studies on the structure and expression of the pheromone genes (C. Miceli and G. Di Giuseppe, personal communication). These studies have established that *E. raikovi* cells, in addition to synthesizing the standard pheromone membrane form, also synthesize its less-represented and "truncated" copy with a mass of nearly 12 kDa (as deduced from its coding nucleotide sequence), i.e., closely matching the mass of the protein responsible for one of the two minor bands revealed by the affinity material (Figure 3). This copy diverges from standard E*r*-1mem only at the level of the intracellular domain, which is shorter by a 17-amino-acid segment and carries numerous and potentially significant substitutions.

Further support for this interpretation was derived from immunoprecipitation analysis of protein complexes stabilized by chemical cross-linking in cell membrane preparations incubated with [^{125}I]E*r*-1. As shown in Figure 4B, anti-1p25/39 antibodies (which are specific for the intracellular side of E*r*-1mem) recognize only the quantitatively more-represented species of radiolabeled complexes of 35–40 kDa, which are consistent with an association between p15 and [^{125}I]E*r*-1 in either a 2:1 or 2:2 ratio and do not bind to the other minor species of complexes consistently with the presumed participation of truncated p15 at their formation.

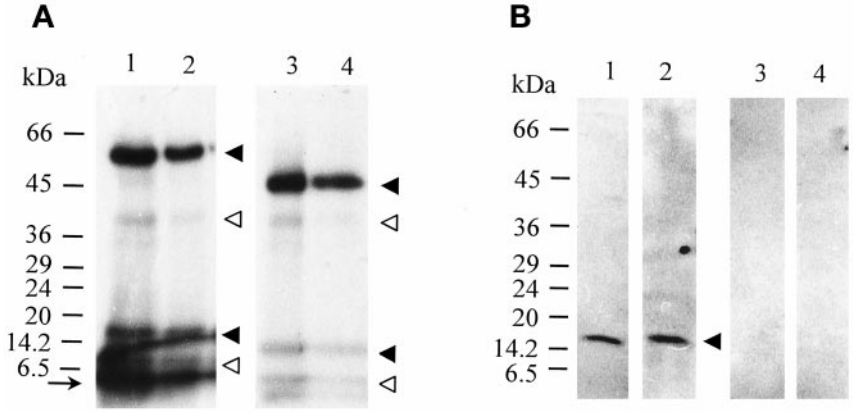

Figure 3. Only p15 of the affinity-purified material is recognized by anti-E*r*-1 and anti-1p25/39 antibodies. In this and the following figures, the positions of molecular mass markers are reported on the left, and the dye front is indicated with an arrow. (A) Affinity material was radioiodinated, run in different amounts (equivalent to 100,000 cpm [lanes 1 and 3] and 60,000 cpm [lanes 2 and 4]) on SDS-PAGE under reducing and nonreducing conditions (lanes 1–2, and 3–4, respectively), and gels were exposed to autoradiography. Major components of 55 and 15 kDa are indicated by filled arrowheads, and minor components of 40 and 12 kDa are indicated by by open arrowheads. (B) Affinity material was analyzed by immunoblotting with anti-E*r*-1 antibodies in the absence and presence of E*r*-1 (16 μM; lanes 1 and 3, respectively) and with anti-1p25/39 antibodies in the absence and presence of the peptide 1p25/39 (16 μM; lanes 2 and 4, respectively). Recognition of p15 is indicated by a filled arrowhead.

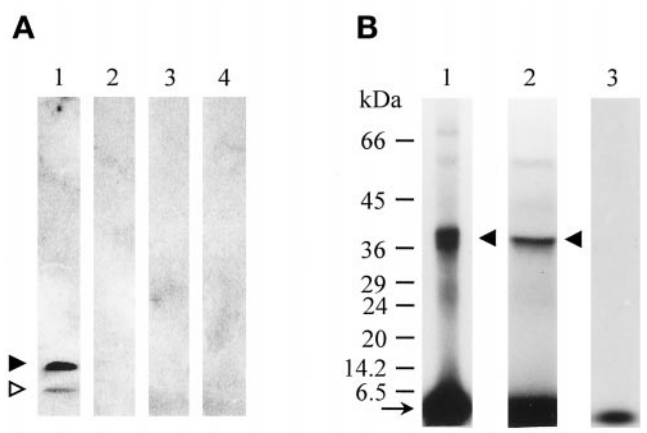

Figure 4. Protein p15 forms complexes with E*r*-1 that are recognized by anti-1p25/39 antibodies. (A) Affinity material was assayed in ligand blotting with [^{125}I]E*r*-1 (0.1 μM, 1.9×10^6 cpm/ml; lane 1), [^{125}I]E*r*-1 plus E*r*-1 (16 μM; lane 2), [^{125}I]E*r*-1 plus E*r*-2 (16 μM; lane 3), and [^{125}I]E*r*-1 after incubation of blotted filters with anti-E*r*-1 antibodies (lane 4). The major band reflecting binding of [^{125}I]E*r*-1 to p15 is indicated by a filled arrowhead; a minor band reflecting binding of [^{125}I]E*r*-1 to a 12-kDa protein, likely representing a truncated form of p15 (see RESULTS), is indicated by an open arrowhead. (B) A cell membrane preparation (protein concentration, 1 mg/ml) was incubated with [^{125}I]E*r*-1 (45 nM, 6.3×10^5 cpm/ml) and exposed to chemical cross-linking with 1-ethyl-3-(3-dimethylaminopropyl) carbodiimide hydrochloride. Cross-linked complexes were then fractionated on SDS-PAGE before (lane 1) or after immunoprecipitation with anti-1p25/39 antibodies in the absence and presence of the peptide 1p25/39 (100 μM; lanes 2 and 3, respectively). Detected and immunoprecipitated protein complexes of 38 kDa are indicated by filled arrowheads.

Characterization of the 55-kDa Protein Copurified with p15

As shown in Figure 3A, p15 is released from the affinity chromatography together with another major protein species of 55 kDa. This protein has been further characterized, and its basic biochemical properties are described here, because they add useful information for a better understanding of the p15 activity.

This characterization of the 55-kDa protein was made easier by the knowledge, summarized in the following three points (from our unpublished results), of the effects generated on *E. raikovi* by cholera toxin (an enzyme that blocks GTP-binding regulatory proteins in their active conformation) and by guanosine 5′-3-*O*-(thio)triphosphate (GTPγS; a GTP analogue that prevents a membrane receptor from interacting with a GTP-binding protein and thus greatly reduces its binding affinity for a ligand): 1) addition of cholera toxin (at micromolar concentrations) to the medium of cells conditioned to enter a new period of vegetative proliferation (after removal from starvation medium and resuspension with food) determines a marked amplification of the rates of [^{3}H]thymidine into the nuclear DNA of these cells; 2) incubation of cell membrane preparations with activated cholera toxin and [^{32}P]NAD reveals that a protein of ~55 kDa is the major substrate for ADP ribosylation; and 3) addition of GTPγS to cell membrane preparations determines a dose-dependent decrease, up to a complete inhibition (at micromolar concentrations), of the pheromone binding to these preparations.

An obvious indication thus emerged from these experimental data, i.e., that a GTP-binding protein is involved in the autocrine mitogenic loop of *E. raikovi*. Based on this indication, we tentatively identified this presumptive protein with the 55-kDa protein copurified with p15 and assessed this assumption, first, by probing samples of the affinity material, after fractionation on SDS-PAGE, with antibodies "anti-GA/1," i.e., raised against the synthetic peptide GA/1 corresponding to the strictly conserved GTP binding site of the α subunit of trimeric GTP-binding (G) proteins (Goldsmith *et al.*, 1988; Mumby and Gilman, 1991). As shown in Figure 5A, these antibodies recognized the 55-kDa protein, and the specificity of this recognition was proven by the fact that their binding to this protein was abolished by the addition of the peptide GA/1 to the incubation mixture. On the other hand, the 55-kDa protein was not recognized by any one of the following other antibodies specific for conserved motifs in the C terminus of G protein α subunits, i.e., anti-$G_{i\alpha\text{-}3}$, anti-$G_{s\alpha}$, anti-$G_{i\alpha\text{-}3}/G_{0\alpha}$, and anti-$G_{i\alpha\text{-}1}/G_{i\alpha\text{-}2}$.

Additional evidence that the 55-kDa protein shares basic functional properties in common with the α subunit of eukaryotic G proteins was derived from analysis of the effects of activated cholera toxin on the affinity material. As shown in Figure 5B, this incubation causes ADP ribosylation of the 55 kDa protein, and, as is the case for the α subunit of stimulatory G proteins (Bornancin *et al.*, 1993), the catalytic effects of the toxin appear to be markedly inhibited (from 30 to 50%, as measured in densitometric analysis of the relative radiograms) by the addition of GTPγS to the incubation mixtures.

Next, it was verified whether the association of the 55-kDa protein with p15 is reversible and GTP mediated. Affinity columns with matrix-bound E*r*-1 were loaded with membrane preparations either not incubated (as usual) with GTPγS or previously incubated with GTPγS; then they were eluted with GTP in carbonate buffer. As shown in Figure 5C, in the former case the eluate contained the 55-kDa protein, whereas in the latter this protein was not detected. The specificity of the GTP effect on the elution of the 55-kDa protein was further supported by the fact that no protein was eluted when GTP was replaced by ATP.

Last, [α-^{32}P]GTP was used to elute affinity columns, and the material eluted was exposed to UV rays for triggering its cross-linking with [α-^{32}P]GTP, according to the procedure of Im and Graham (1990). The results of the electrophoretic and autoradiographic analysis of the radiolabeled complexes formed are shown in Figure 5D. It appears that [α-^{32}P]GTP is effectively linked by the 55-kDa protein into complexes that are specifically recognized by anti-GA/1 antibodies. Also, two other minor species of radiolabeled complexes of ~18 and 38 kDa were usually visualized by this analysis; however, they are not immunorecognized and presumably represent breakdown products of the larger 55-kDa complexes.

Activity of Recombinant Domains of p15

To provide direct evidence that the extracellular and cytoplasmic domains of p15 are intrinsically and independently competent to bind, respectively, pheromones and the 55-

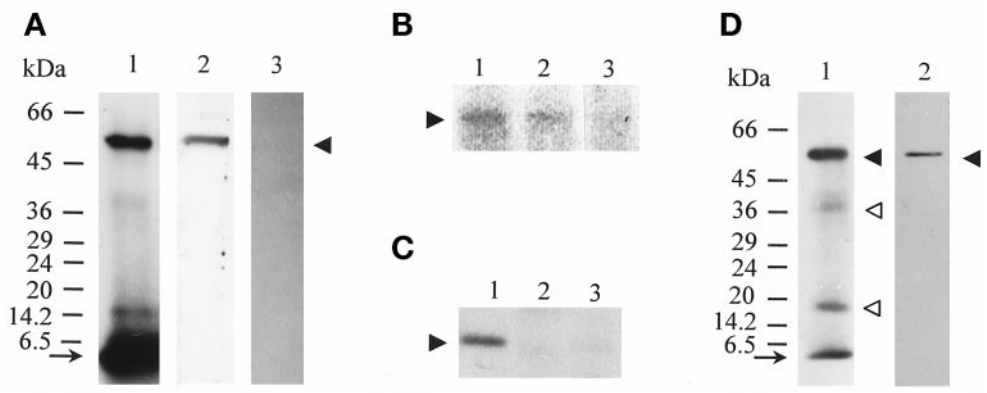

Figure 5. The 55-kDa protein, copurified with p15, is recognized by anti-GA/1 antibodies, is ADP-ribosylated by cholera toxin, and binds GTP. (A) Affinity material was either radioiodinated and analyzed by electrophoresis and autoradiography as in Figure 3 (lane 1) or analyzed by immunoblotting with anti-GA/1 antibodies in the absence and presence of peptide GA/1 (40 μM; lanes 2 and 3, respectively). Recognition of the 55-kDa protein is indicated by a filled arrowhead. (B) Affinity material was incubated either with activated cholera toxin and [^{32}P]NAD, in the absence and presence of GTPγS (0.1 mM; lanes 1 and 2, respectively), or only with [^{32}P]NAD (lane 3), fractionated on SDS-PAGE, and gels were scanned for radioactivity with a molecular imager system. The radiolabeled 55-kDa protein is indicated by a filled arrowhead. (C) Material was either eluted with GTP (0.1 mM in the presence of 0.5 mM $MgCl_2$) from affinity chromatography loaded with membrane preparations previously not incubated or incubated with GTPγS (0.1 mM; lanes 1 and 2, respectively) or with ATP (0.1 mM in the presence of 0.5 mM $MgCl_2$) from affinity chromatography loaded with membrane preparations not incubated with GTPγS (lane 3), and then analyzed by immunoblotting with anti-GA/1 antibodies. The 55-kDa protein detected in lane 1, and not detected in the two other lanes, is indicated by a filled arrowhead. (D) Material was eluted with [α-^{32}P]GTP (16 nM, 3000 Ci/mmol) from affinity chromatography, exposed to UV irradiation, fractionated on SDS-PAGE, and blotted onto polyvinylidene difluoride filters. Blotted filters were then exposed to autoradiography (lane 1) or incubated with anti-GA/1 antibodies (lane 2). Complexes between [α-^{32}P]GTP and the 55-kDa protein are indicated by filled arrowheads; two other minor species of radiolabeled complexes, not recognized by anti-GA/1 antibodies, are indicated by open arrowheads.

kDa protein, the sequences of these domains were generated as recombinant proteins to be used separately in analysis of their activities. Their construction (see Figure 1) was made without addition of any extraneous amino acids to their native sequences and with the p15 transmembrane segment (corresponding to the pre segment of prepro-E*r*-1) in common: the sequence of protein containing p15 extracellular domain, denoted p143, spanning from Met^{56} to Val^{130}; and that of protein containing p15 cytoplasmic domain, denoted p3/10, spanning from Met^{1} to Ala^{74}. Both p143 and p3/10 were expressed through the IMPACT system, based on the excision of the intein self-cleavage site for the release of the relative target products. Although p3/10 was used in a form covalently linked to intein-CBD molecules through Ala^{74} (and, hence, with a topological orientation equivalent to that in p15), p143 was used after cleavage from these molecules. For improving p143 solubility during purification, guanidine was applied to chitin columns (as suggested by the manufacturer). As a consequence, p143 coeluted with some intein-CBD molecules. These, however, were effectively removed together with guanidine by a single purification step on reversed phase chromatography, so that homogeneous preparations of p143 proteins were eventually obtained, as assessed by immunoblot analysis (our unpublished results).

After transfer onto nitrocellulose filters, p143 was probed in ligand-blotting experiments with [^{125}I]E*r*-1. As shown in Figure 6A, autoradiography of these filters revealed effective radioligand binding to p143, and the specificity of this binding was proven by causing its complete inhibition by adding excess of E*r*-1, or other pheromones that compete with E*r*-1, to the incubation mixtures.

The construct p3/10-intein-CBD was used as a matrix of affinity columns, which were then loaded with membrane preparations and eluted with GTP. As shown in Figure 6B, three bands were usually revealed by the material eluted from these columns and analyzed in immunoblotting with anti-GA/1 antibodies. However, only the band at 55 kDa appeared to be generated by a protein associated with the affinity matrix through p3/10 and recognized in a specific manner. The other two bands were in fact present also in material eluted from affinity columns containing, as control, intein-CBD molecules without p3/10, and, differently from the 55-kDa band, their formation was not inhibited after incubation of blotted filters with excess of peptide GA/1.

DISCUSSION

The results that we have described provide evidence that 1) E*r*-1mem is the only membrane protein to which type I cells of *E. raikovi* have committed the function of pheromone binding site, and 2) the same protein is a good candidate for assuming also the function of effective pheromone receptor, capable of signaling the effects generated by its ligand binding activity. The recognition of these properties for E*r*-1mem raises the questions of how this protein, and equivalent proteins that are likely synthesized by the other many cell types that represent *E. raikovi*, can bind their partner soluble forms homotypically as well as nonpartner pheromones heterotypically and, accordingly, promote cell vegetative reproduction or mating.

For addressing the former question, we can rely on the determination of the molecular packing of E*r*-1 in the crystal

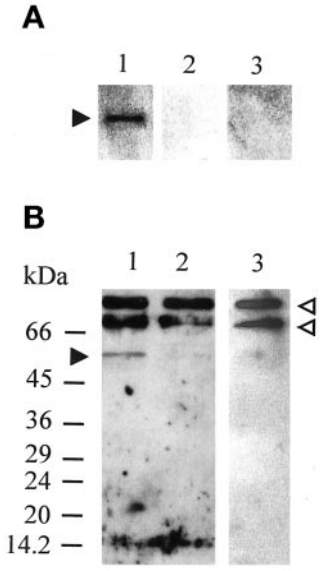

Figure 6. Protein p143 binds E*r*-1, and protein p3/10 binds the 55-kDa protein. (A) Samples of p143 were assayed by ligand blotting with [^{125}I]E*r*-1 (0.1 μM, 1.9 $\times$ 10^6 cpm/ml; lane 1), with [^{125}I]E*r*-1 plus E*r*-1 (16 μM; lane 2), or with [^{125}I]E*r*-1 plus E*r*-2 (16 μM; lane 3). A filled arrowhead indicates [^{125}I]E*r*-1 binding to p143. (B) Material was eluted with GTP from affinity chromatography set up with cell membrane preparations loaded on chitin columns carrying either p3/10 linked to intein-CBD molecules (lane 1) or intein-CBD molecules without p3/10 (lane 2) and then analyzed by immunoblotting with anti-GA/1 antibodies. Recognition of the 55-kDa protein is indicated by a filled arrowhead. Other proteins that are released from both columns and recognized in a nonspecific manner, because they do not disappear after addition of peptide GA/1 (40 μM) to the incubation mixture with anti-GA/1 antibodies (lane 3), are indicated by open arrowheads.

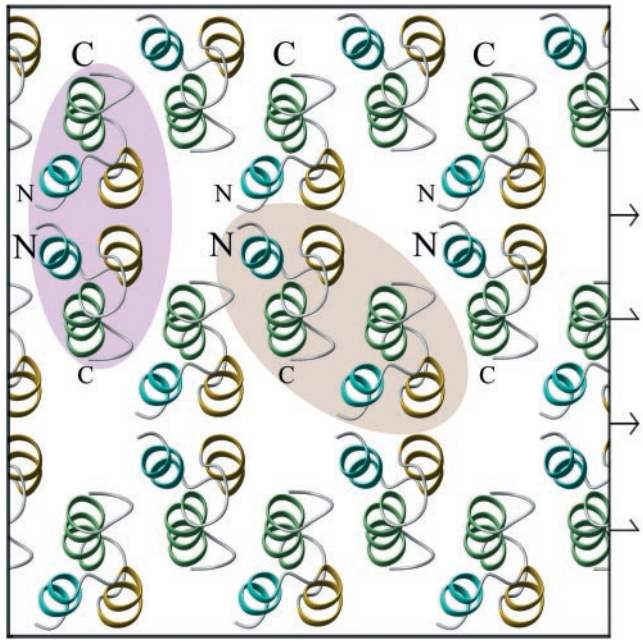

Figure 7. Cooperative model of E*r*-1–E*r*-1mem interactions. The model is modified from the study of the E*r*-1 crystal structure by Weiss *et al.* (1995), and the representation was prepared by using the MOLMOL program (Koradi *et al.*, 1996). On the basis of the structural similarity of the extracellular domain of E*r*-1mem with E*r*-1, it is assumed that E*r*-1–E*r*-1mem interactions on the cell surface mimic E*r*-1–E*r*-1 interactions in the crystal lattice. Half of the molecules are top viewed, with their N termini in the back and C termini in the front; they represent E*r*-1mem molecules on the cell surface. The other half are bottom viewed, with their N termini in the front and C termini in the back; they represent soluble E*r*-1 molecules. Back and front positions are indicated by smaller and larger letters, respectively. The two types of dimeric associations that each molecule can form with its neighboring molecules are outlined by ovals of different colors. Positions of the twofold rotation axes between molecules in dimers 1 and the twofold screw axes between molecules in dimers 2 are indicated on the margin by symmetrical and asymmetrical arrows, respectively.

structure (Weiss *et al.*, 1995) and the nuclear magnetic resonance solution structures of the same pheromone E*r*-1 and its binding competitors, E*r*-2, E*r*-10, and E*r*-11 (Brown *et al.*, 1993; Luginbühl *et al.*, 1994, 1996). The knowledge of the E*r*-1 crystal structure has allowed the definition of a molecular model just based on the rationale that, in the two-dimensional array of the cell surface, E*r*-1mem–E*r*-1 interactions mimic (because of the structural equivalency of these proteins) the E*r*-1–E*r*-1 interactions that have been resolved in the x–y plane of the crystal (Weiss *et al.*, 1995). In this model, reproduced in Figure 7, effective and increasingly tight E*r*-1mem–E*r*-1 binding derives from a process of cooperative protein–protein oligomerization, which uses initially weak association energies and arranges the molecules into layers. These energies arise from the participation of the interacting molecules, with all their three helices and the three faces (A–C) that these helices delimit, in the formation of two types of dimers, denoted dimers 1 and 2, neither of which can apparently form in solution because of relatively small areas buried in their formation. Dimers 1 are symmetrical structures between two molecules that bury their mainly hydrophobic face A to form a four-helical bundle composed of helices 1 and 2 from both monomers. Dimers 2 are linear structures without symmetrical contacts between two molecules that are related by a twofold screw axis and stack their helix 3 in an antiparallel manner to form preeminently hydrophilic interactions between their faces B and C (both convergent into helix 3).

An assessment of whether this cooperative model of homotypic binding between E*r*-1mem and its partner molecule E*r*-1 can hold also for the heterotypic binding (responsible for cell mating induction) of E*r*-1mem with other nonpartner pheromones has been based on a comparison of the backbone molecular conformation and electrostatic surface potential of E*r*-1 with their respective counterparts determined in E*r*-2, E*r*-10, and E*r*-11. As illustrated in Figure 8, all these molecules show their face A, which is completely involved in the formation of type 1 dimers, similarly shaped and substantially uncharged. Thus, E*r*-1mem would appear able to associate with any one of pheromones E*r*-2, E*r*-10, or E*r*-11 according to the dimer 1 pattern. Different is the situation for faces B and C, both largely involved in the formation of type 2 dimers. In this case, obvious specificities of shape and potential distinguish pheromones from one another to var-

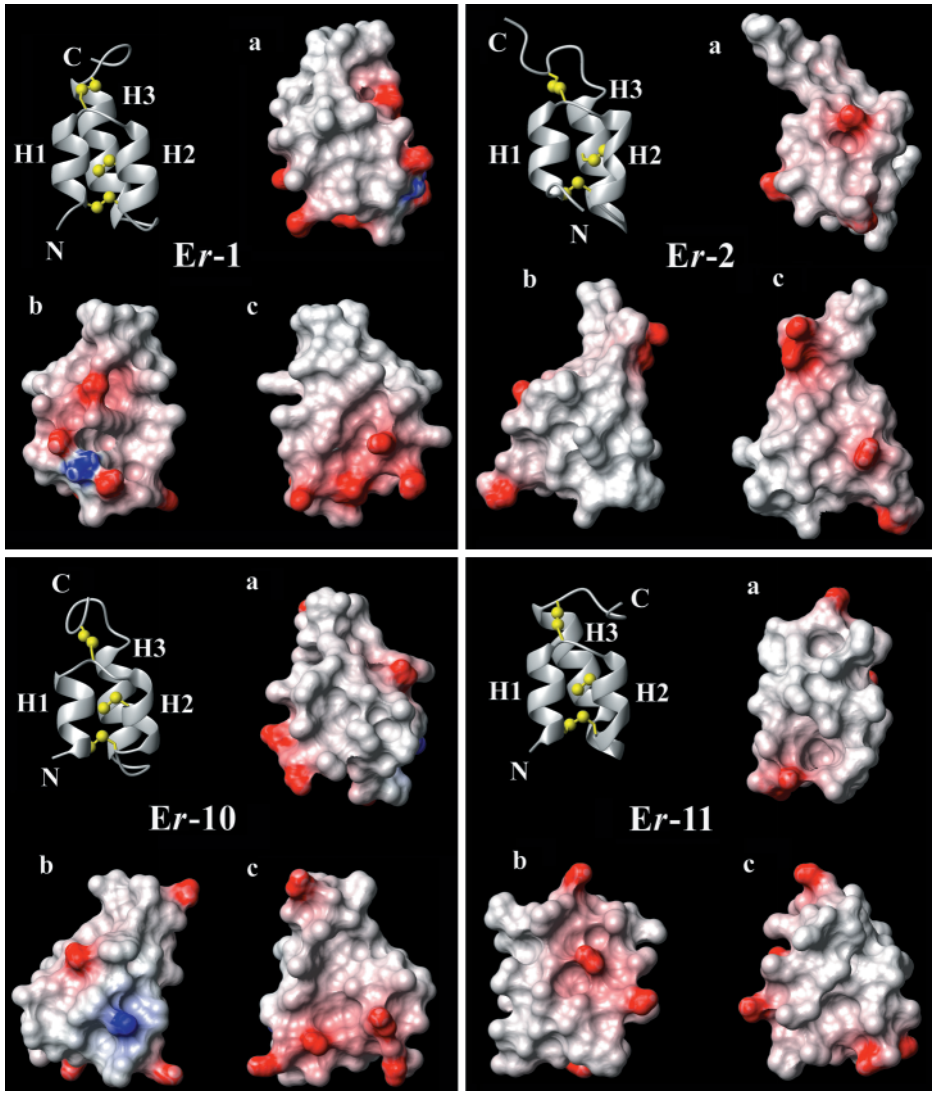

Figure 8. Comparison of pheromone structures. In the ribbon representations of pheromones Er-1, Er-2, Er-10, and Er-11, the three helices are denoted H1, H2, and H3, and the six sulfur atoms involved in the three conserved disulfide bonds are represented as gold spheres. For each pheromone is shown the overall distribution of the electrostatic potentials on the three faces, indicated by a–c, and delimited by H1 and H2, H2 and H3, and H1 and H3, respectively. Neutral, negative, and positive potentials are coded white, red, and blue, respectively. Both ribbon and surface potential representations were prepared by using the MOLMOL program (Koradi *et al.*, 1996), with standard charge settings, and are drawn to scale.

ied degrees. In Er-1, both faces are locally charged because of clusters of three residues of Glu and one of Arg in face B and two of Glu and two of Asp in face C. In the other pheromones, the same faces are either markedly less charged or nearly uncharged, with the exception of face C of Er-10, which maintains a cluster of two Glu and two Asp residues. Thus, the capacity of Er-1mem to form heterotypic pheromone associations of the type 2 dimer is presumably effectively modified. These modifications might then restrict or abolish, depending on the protein–protein combination, the dynamics of the cooperative oligomerization that distinguishes Er-1mem–Er-1 interactions and in turn cause an interruption of the cell growth signal generated by this oligomerization in the autocrine loop. In effect, attempts to obtain crystals from mixtures of Er-1 and Er-2 molecules have so far failed (D. Anderson and D. Eisenberg, personal communication), and further restrictions to a cooperative oligomerization of Er-1mem with nonpartner pheromones might also be produced by structural specificities that pheromones show in the conformation of their helix 2 involved in the formation of both types of dimers (Luginbühl *et al.*, 1994, 1996; Weiss *et al.*, 1995).

In relation to the question of the signaling capacity of Er-1mem, there is primary interest in determining the structure of the GTP-binding protein of 55 kDa that has been found associated with the Er-1mem intracellular domain. We expect to know from this determination whether structure–function relationships link this protein to the α-subunit of G proteins. Er-1mem does not possess the seven-helix membrane-spanning organization typical of cell receptors that work coupled to these regulatory proteins, and it is strongly debated (Korner *et al.*, 1995) the identification of unusual G protein-coupled receptors represented by single-pass transmembrane proteins (Telfer and Rudd, 1991; Nishimoto *et al.*, 1993; Okamoto *et al.*, 1995; Goretzki and Mueller, 1998). Nevertheless, in an analysis with the PROSITE database (Bairoch, 1993), the cytoplasmic domain of Er-1mem reveals two adjacent segments, one spanning from Ser^{27} to

Ser[42] and the other spanning from Ser[42] to Lys[58], which bear a similarity of 82 and 73%, respectively, with a sequence generally recognized as a "G-protein coupled receptor signature" (Attwood *et al.*, 1991). In addition, in a position extending into the transmembrane domain, the intracellular side of E*r*-1mem contains the motif Arg-Met-Asn-Lys recalling that BBXXB (where B and X stand for a basic and any amino acid residues, respectively), indicated as a feature distinctive of a G protein activating domain (Okamoto *et al.*, 1991; Ikezu *et al.*, 1992; Nishimoto *et al.*, 1993; Pennington, 1995).

Still germane to the signaling activity of E*r*-1mem, there is also in vivo evidence that antibody-mediated clustering of these molecules promotes cell mitogenic activity (Vallesi *et al.*, 1995), and two potential phosphorylation sites for protein kinases A and C, represented by the canonical motif Arg/Lys-X-X-Ser (Kennelly and Krebs, 1991), are present in the E*r*-1mem cytoplasmic domain. A pheromone binding-dependent phosphorylation at these sites might regulate E*r*-1mem activity, either in concert with or independently of the 55-kDa protein; likewise, numerous G protein-coupled receptors are inactivated and internalized after phosphorylation of their intracellular side by specific kinases (Rockman *et al.*, 1996; Zhang *et al.*, 1997; Carman and Benovic, 1998).

So far, E*r*-1mem has been considered only in relation to its activity as cell pheromone binding site and signaling receptor. However, the structural equivalence of the extracellular domain of this membrane protein with its partner soluble pheromone clearly suggests that E*r*-1mem may also carry out ligand functions. This multifunctionality has been documented for other transmembrane proteins, such as those representing CD21 and CD23 ligand–receptor systems of some hematopoietic cell types (Gordon *et al.*, 1989; Aubry *et al.*, 1992), and is increasingly appreciated for numerous growth factors belonging mostly to the epidermal growth factor and tumor necrosis factor α protein families (Massagué, 1990; Massagué and Pandiella, 1993; Singer, 1992). Instead of being proteolytically processed and released into the extracellular environment as usually occurs, these soluble growth factors can be inserted into the plasma membrane and exposed on the cell surface, to allow juxtacrine cell interactions between physically contacting cells (Bosenberg and Massagué, 1993). The binding of E*r*-1mem molecules directly with one another across the extracellular space between facing cell membranes, for promoting transient intercellular communication and adhesion for mating pair formation, appears to be strongly supported by a comparative analysis of the energetics of oligomerization shown by E*r*-1 in solution and in the crystal lattice (Weiss *et al.*, 1995). In essence, this analysis reveals that the efficiency of binding of E*r*-1 is thermodynamically greatly improved if these molecules were to be partially immobilized in a plane. Such a planar arrangement in fact reflects the disposition of E*r*-1mem in the cell membrane.

ACKNOWLEDGMENTS

We are grateful to Drs. D. Anderson, R.A. Bradshaw, D. Eisenberg, and J. Kloetzel who provided very helpful comments and suggestions on the manuscript. This work was supported by grants to P.L. from the Italian Ministero dell'Universitá e della Ricerca Scientifica e Tecnologica and Consiglio Nazionale delle Ricerche.

REFERENCES

Attwood, T.K., Eliopoulos, E.E., and Findlay, B.C. (1991). Multiple sequence alignment of protein families showing low sequence homology: a methodological approach using database pattern-matching discriminators for G-protein-linked receptors. Gene *98*, 153–159.

Aubry, J.-P., Pochon, S., Graber, P., Jansen, K.U., and Bonnefoi, J.-Y. (1992). CD21 is a ligand for CD23 and regulates IgE production. Nature *358*, 505–507.

Bairoch, A. (1993). The PROSITE dictionary of sites and patterns in proteins, its current status. Nucleic Acids Res. *21*, 3097–3103.

Beale, G.H. (1990). Self and nonself recognition the ciliate protozoan *Euplotes*. Trends Genet. *6*, 137–139.

Bornancin, F., Audigier, Y., and Chabre, M. (1993). ADP-ribosylation of G_s by cholera toxin is potentiated by agonist activation of beta-adrenergic receptors in the absence of GTP. J. Biol. Chem. *268*, 17026–17029.

Bosenberg, M.W., and Massagué, J. (1993). Juxtacrine cell signaling molecules. Curr. Opin. Cell Biol. *5*, 832–838.

Brown, L.R., Mronga, S., Bradshaw, R.A., Ortenzi, C., Luporini, P., and Wüthrich, K. (1993). Nuclear magnetic resonance solution structure of the pheromone E*r*-10 from the ciliated protozoan *Euplotes raikovi*. J. Mol. Biol. *231*, 800–816.

Carman, V.C., and Benovic, J.L. (1998). G-protein-coupled receptors: turn-ons and turn-offs. Curr. Opin. Neurobiol. *8*, 335–344.

Concetti, A., Raffioni, S., Miceli, C., Barra, D., and Luporini, P. (1986). Purification to apparent homogeneity of the mating pheromone of *mat-1 Euplotes raikovi*. J. Biol. Chem. *61*, 10582–10587.

Goldsmith, P., Rossiter, K., Carter, A., Simonds, W., Unson, C.G., Vinitisky, R., and Spiegel, A.M. (1988). Identification of the GTP-binding protein encoding by G_{i3} complementary DNA. J. Biol. Chem. *263*, 6476–6479.

Gordon, J., Flores-Romo, L., Cairns, J.A., Millsum, M.J., Lane, P.J., Johnson, G.D., and McLennan, I.C.M. (1989). CD23: a multi-functional receptor/linphokine? Immunol. Today *10*, 153–157.

Goretzki, L., and Mueller, B.M. (1998). Low-density-lipoprotein-receptor-related protein (LRP) interacts with a GTP-binding protein. Biochem. J. *336*, 381–386.

Heckmann, K., and Kuhlmann, H.W. (1986). Mating types and mating inducing substances in *Euplotes octocarinatus*. J. Exp. Zool. *237*, 87–96.

Ikezu, T., Okamoto, T., Ogata, E., and Nishimoto, I. (1992). Amino acids 356–372 constitute a G_i-activator sequence of the alpha 2-adrenergic receptor and have Phe substitute in the G protein-activator sequence motif. FEBS Lett. *311*, 29–32.

Im, M.J., and Graham, R.M. (1990). A novel guanine nucleotide-binding protein coupled to the α_1-adrenergic receptor. J. Biol. Chem. *265*, 18944–18951.

Kennelly, P., and Krebs, E.G. (1991). Consensus sequence as substrate specificity determinants for protein kinase and protein phosphatase. J. Biol. Chem. *266*, 1555–1558.

Koradi, R., Billeter, M., and Wüthrich, K. (1996). MOLMOL: a program for display and analysis of macromolecular structures. J. Mol. Graph. *14*, 51–55.

Korner, C., Nurnberg, B., Uhde, M., and Braulke, T. (1995). Mannose 6-phosphate/insulin-like growth factor II receptor fails to interact with G-proteins. J. Biol. Chem., *270*, 287–295.

Kuhlmann, H.V., and Heckmann, K. (1989). Adolescence in *Euplotes octocarinatus*. J. Exp. Zool. *251*, 316–328.

La Terza, A., Miceli, C., and Luporini, P. (1995). Differential amplification of pheromone genes of the ciliate *Euplotes raikovi*. Dev. Genet. *17*, 272–279.

Luginbühl, P., Ottiger, M., Mronga, S., and Wüthrich, K. (1994). Structure comparison of the pheromones Er-1, Er-10, and Er-2 from *Euplotes raikovi*. Protein Sci. *3*, 1537–1546.

Luginbühl, P., Wu, J., Zerbe, O., Ortenzi, C., Luporini, P., and Wüthrich, K. (1996). The NMR solution structure of the pheromone Er-11 from the ciliated protozoan *Euplotes raikovi*. Protein Sci. *5*, 1512–1522.

Luporini, P., and Miceli, C. (1986). Mating pheromones. In: The Molecular Biology of Ciliated Protozoa, ed. J.D. Gall, New York: Academic Press, 263–299.

Luporini, P., Miceli, C., Ortenzi, C., and Luporini, P. (1996). Ciliate Pheromones. In: Signaling Mechanisms in Protozoa and Invertebrates, ed. G. Csaba and W.E.G. Müller, Berlin: Springer, 80–104.

Luporini, P., Miceli, C., Ortenzi, C., and Vallesi, A. (1992). Developmental analysis of the cell recognition mechanism in the ciliate *Euplotes raikovi*. Dev. Genet. *13*, 9–15.

Luporini, P., Miceli, C., Vallesi, A., and Bradshaw, R.A. (1995). Chemical signaling in ciliates. J. Eukaryot. Microbiol. *42*, 208–212.

Luporini, P., Raffioni, S., Concetti, A., and Miceli, C. (1986). The ciliate *Euplotes raikovi* heterozygous at the *mat* genetic locus coreleases two individual species of mating pheromones: genetic and biochemical evidence. Proc. Natl. Acad. Sci. USA *83*, 2889–2893.

Massagué, J. (1990). Transforming growth factor-α: a model for membrane-anchored growth factors. J. Biol. Chem. *265*, 21393–21396.

Massagué, J., and Pandiella, A. (1993). Membrane-anchored growth factors. Annu. Rev. Biochem. *62*, 515–541.

Miceli, C., La Terza, A., Bradshaw, R.A., and Luporini, P. (1991). Structural characterization of mating pheromone precursors of the ciliate protozoan *Euplotes raikovi*. Eur. J. Biochem. *202*, 759–764.

Miceli, C., La Terza, A., Bradshaw, R.A., and Luporini, P. (1992). Identification and structural characterization of a cDNA clone encoding a membrane-bound form of the polypeptide pheromone Er-1 in the ciliate protozoan *Euplotes raikovi*. Proc. Natl. Acad. Sci. USA *89*, 1988–1992.

Miceli, C., La Terza, A., and Melli, M. (1989). Isolation and structural characterization of cDNA clones encoding the mating pheromone Er-1 secreted by the ciliate *Euplotes raikovi*. Proc. Natl. Acad. Sci. USA *86*, 3016–3020.

Miyake, A. (1981). Cell interactions by gamones in *Blepharisma*. In: Sexual Interactions in Eucaryotic Microbes, ed. D.H. O'Day and P. Horgen, New York: Academic Press, 95–129.

Miyake, A. (1996). Fertilization and sexuality in ciliates. In: Ciliates: Cells as Organism, ed. K. Hausmann and P.C. Bradbury, Stuttgart: Gustav Fischer Verlag, 243–290.

Mumby, S.M., and Gilman, A.G. (1991). Synthetic peptide antisera with determined specificity for G protein α or β subunits. Methods Enzymol. *195*, 215–233.

Nishimoto, I., Okamoto, T., Matsuura, Y., Takahashi, S., Okamoto, T., Murayama, Y., and Ogata, E. (1993). Alzheimer amyloid protein precursor complexes with brain GTP-binding protein G_o. Nature *362*, 75–79.

Okamoto, T., Murayama, Y., Inagaki, M., Ogata, E., and Nishimoto, I. (1991). Identification of a G_s activator region of the β2-adrenergic receptor that is autoregulated via protein kinase A-dependent phosphorylation. Cell *67*, 723–730.

Okamoto, T., Takeda, S., Murayama, Y., Ogata, E., and Nishimoto, I. (1995). Ligand-dependent G protein coupling function of amyloid transmembrane precursor. J. Biol. Chem. *270*, 4205–4208.

Ortenzi, C., and Luporini, P. (1995). Competition among homologous polypeptide pheromones of the ciliate *Euplotes raikovi* for binding to each other's cell receptors. J. Eukaryot. Microbiol. *42*, 242–248.

Ortenzi, C., Miceli, C., Bradshaw, R.A., and Luporini, P. (1990). Identification and initial characterization of an autocrine pheromone receptor in the protozoan ciliate *Euplotes raikovi*. J. Cell Biol. *111*, 607–614.

Pennington, S.R. (1995). GTP-binding protein: heterotrimeric G proteins. Protein profile *2*, 167–315.

Raffioni, S., Miceli, C., Vallesi, A., Chowdhury, S.K., Chait, B.T., Luporini, P., and Bradshaw, R.A. (1992). Primary structure of *Euplotes raikovi* pheromones: comparison of five sequences of pheromones with variable mating interactions. Proc. Natl. Acad. Sci. USA *89*, 2071–2075.

Rockman, H.A., Choi, D., Rahman, N.U., Akhter, S.A., Lefkowitz, R.J., and Koch, W.J. (1996). Receptor-specific *in vivo* desensitization by the G protein-coupled receptor kinase-5 in transgenic mice. Proc. Natl. Acad. Sci. USA *93*, 99534–9959.

Singer, S.J. (1992). Intercellular communication and cell-cell adhesion. Science *255*, 1671–1677.

Stewart, A.E., Raffioni, S., Chaudhary, T., Chait, B.T., Luporini, P., and Bradshaw, R.A. (1992). The disulfide bond pairing of the pheromones Er-1 and Er-2 of the ciliate protozoan *Euplotes raikovi*. Protein Sci. *1*, 777–785.

Telfer, J.C., and Rudd, C.E. (1991). A 32-kD GTP-binding protein associated with the CD4–$p556^{lck}$ and CD8–$p56^{lck}$ T cell receptor complexes. Science *254*, 439–441.

Vallesi, A., Giuli, G., Bradshaw, R.A., and Luporini, P. (1995). Autocrine mitogenic activity of pheromones produced by the protozoan ciliate *Euplotes raikovi*. Nature *376*, 522–524.

Vallesi, A., Giuli, G., Ghiara, P., Scapigliati, G., and Luporini, P. (1998). Structure-function relationships of pheromones of the ciliate *Euplotes raikovi* with mammalian growth factors: cross-reactivity between Er-1 and interleukin-2 systems. Exp. Cell Res. *241*, 253–259.

Weiss, M.S., Anderson, D.H., Raffioni, S., Bradshaw, R.A., Ortenzi, C., Luporini, P., and Eisenberg, D. (1995). A cooperative model for receptor recognition and cell adhesion: evidence from the molecular packing in the 1.6-Å crystal structure of the pheromone Er-1 from the ciliated protozoan *Euplotes raikovi*. Proc. Natl. Acad. Sci. USA *92*, 10172–10176.

Zhang, L., Sports, C.D., Osawa, S., and Weiss, E.R. (1997). Rhodopsin phosphorylation sites and their role in arrestin binding. J. Biol. Chem. *272*, 14762–14768.